

I. Abstract

Recently, the high levels of Fecal Indicator Bacteria (FIB) at Huntington Beach, CA, have been a motivation for study of the nearshore coastal processes in the area. The goal has been to identify possible sources of the contamination. In this study, we build a 2-D model of an off-shore transect of Huntington Beach that combines the effects of the M2 internal tide and wind stress due to the diurnal seabreeze to elucidate their effect on cross-shore transport. The model positively compares with velocity profiles measured in the area and readily shows the non-linearity of the shoaling internal tides. We calculate shoreward advection with the horizontal position of the pycnocline. This study shows that the interaction of wind stress and internal tides is dependent on the phase between the two forcings. In general, the interaction limits the shoreward advection of the pycnocline.

Fig. 1 : The Numerical Domain

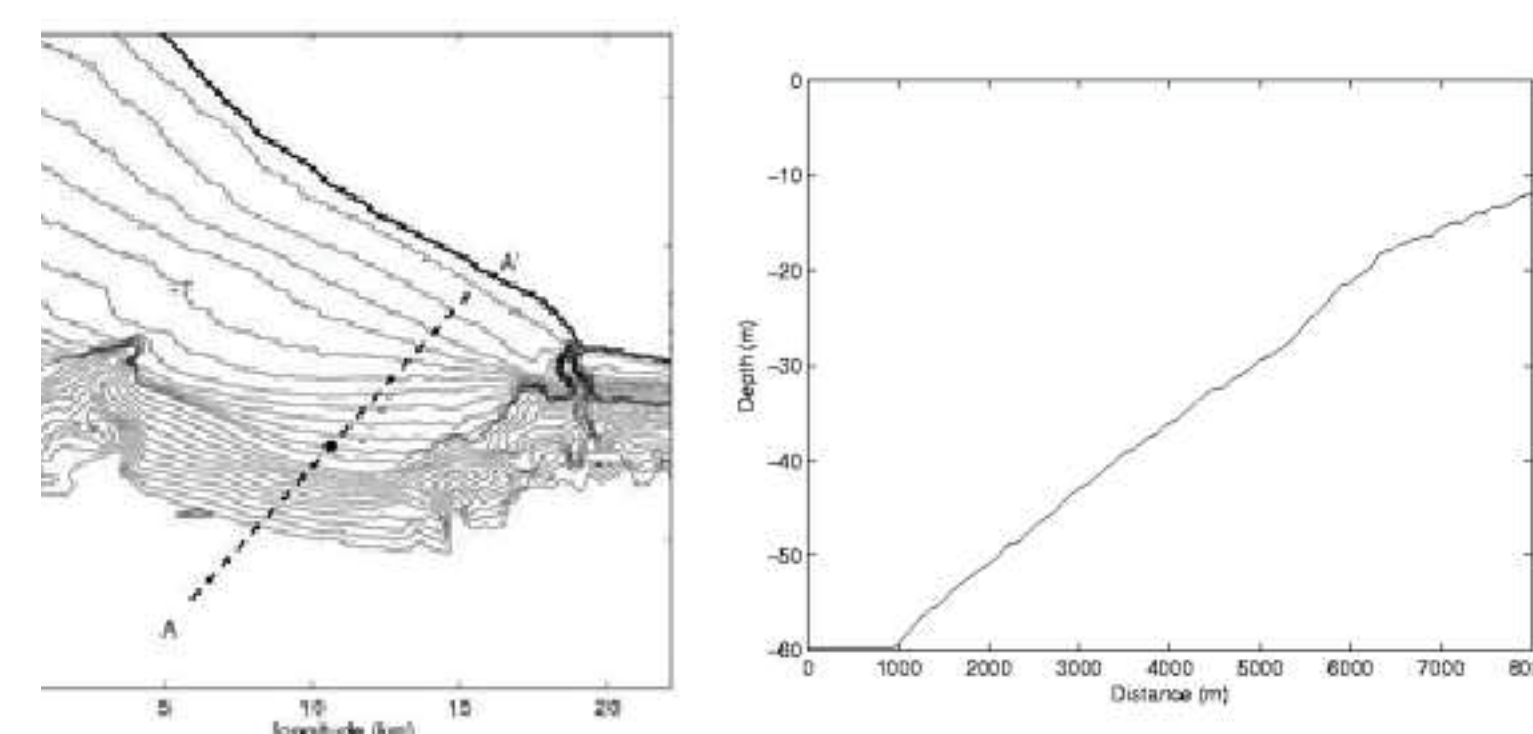


Fig. 1 : The transect (left) and the numerical domain (right) that was created along it for simulation. The point at A' is the right hand wall of the domain, which then extends 7 km out the transect. The kilometer of constant depth on the left forms the numerical sponge-layer.

II. Model Setup

We implemented a no-slip boundary condition on the bottom and used a free-slip condition on the east boundary. We imposed a sponge layer boundary at the west side of the domain by adding a damping term to the horizontal momentum equation of the form,

$$F_s(x, z, t) = -\frac{u(x, z, t)}{\tau} \exp\left(-\frac{x}{L_D}\right)$$

where $\tau = 7200$ s is the damping timescale and $L_D = 1000$ m is the damping lengthscale. At the free-surface, wind-forcing was included by specifying the surface wind-induced velocity with the form,

$$u^* = W_{amp} \sin(\omega_{wind}t + \phi) + W_{avg}$$

where $W_{amp} = 0.04$ m/s is the magnitude of the surface wind velocity oscillations at the diurnal wind frequency, $\omega_{wind} = 7.27 \times 10^{-5}$ rad/s, $W_{avg} = 0.04$ m/s is the daily average wind speed, and ϕ is the phase lag between the wind forcing and the internal tide. W_{amp} and W_{wind} were calibrated to obtain wind-induced velocities similar to the data presented in Noble et al. [2003], while ϕ was varied to study the effect of the difference in phasing between the winds and tides on transport.

We modeled the tidal action by forcing a first-mode M2 internal tide in the horizontal momentum equation with,

$$F(x, z, t) = F_0 u(z) \sin(\omega_{tide}t) \exp\left(-\left(\frac{x-x_0}{L_c}\right)^2\right)$$

where F_0 is the forcing magnitude, ω_{tide} is the M2 tidal frequency, $u(z)$ is the first-mode internal wave velocity profile, x_0 is the location of the forcing, and L_c is the envelope over which the forcing decays. We adjusted the the forcing to obtain internal wave-induced velocities that are consistent with field measurements, such that $F_0 = 1.75 \times 10^{-5}$ m/s², $x_0 = 1000$ m, and $L_c = 800$ m.

Fig. 2 : Effect of Internal Waves

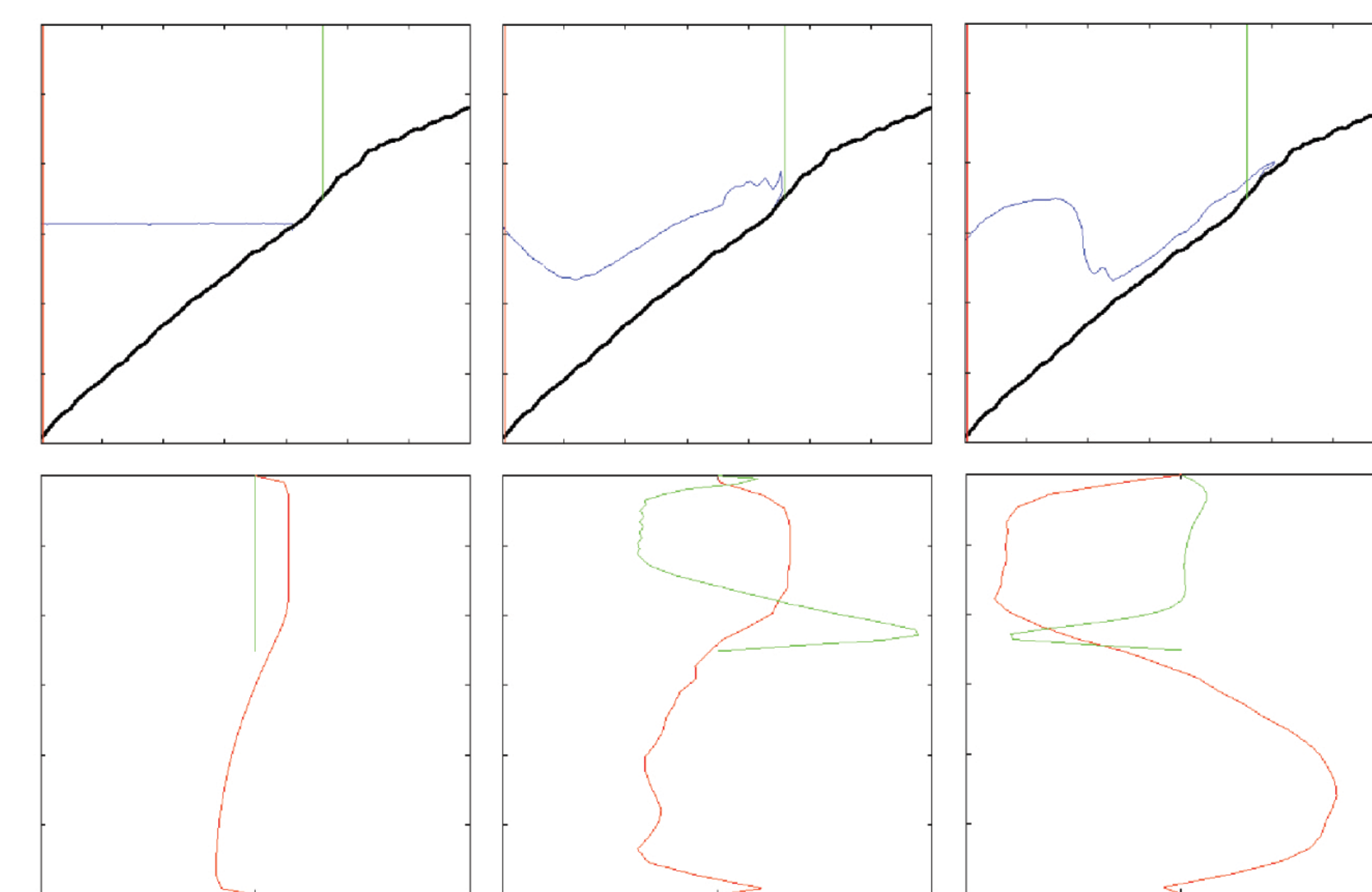


Fig. 2 : The position of the pycnocline and the corresponding velocity profiles for $t = 0, 17.8$ and 24 hrs with normal wave forcing and wind amplitude of 0 . The horizontal range of the pycnocline, 1347 m, confirms that the semi-diurnal internal tide can act as a cross-shelf transport mechanism for sub-thermocline water at Huntington Beach, see Boehm et al. [2002].

We modeled the eddy viscosity using a zero-equation model,

$$\nu_t|_{Bouancy} = \nu_t(z)(1 + \alpha Ri)^\gamma + \nu_0$$

$$\nu_t(z) = \kappa D u^* \left(-\frac{z}{D}\right) \left(1 + \frac{z}{D}\right)$$

where $\alpha = 10$, $\gamma = -.5$, $\kappa = .41$, D is the depth at bottom where the viscosity is being calculated, and u^* is the prescribed wind friction velocity. The background viscosity, ν_0 , was 3×10^{-4} . Again, those parameters were calibrated to obtain results similar to those in Noble et. al. The initial conditions were a quiescent stratified fluid using stratification data consistent with measurements from the field.

III. Simulation Results

We ran the simulations for 48 hours a run, with a time step of 40 s, enough time for the wind stress to effect the internal wave action. Twenty four simulations were carried out for values of ϕ , the phase difference, in order to study the its effects on the maximum shoreward penetration of the pycnocline. We found the position of the pycnocline, defined as $\Delta\rho/\rho = 3.5 \times 10^{-4}$, and define the point of maximum shoreward penetration of the pycnocline as X_{max} .

Fig. 3 : Effect of Wind - Forcing

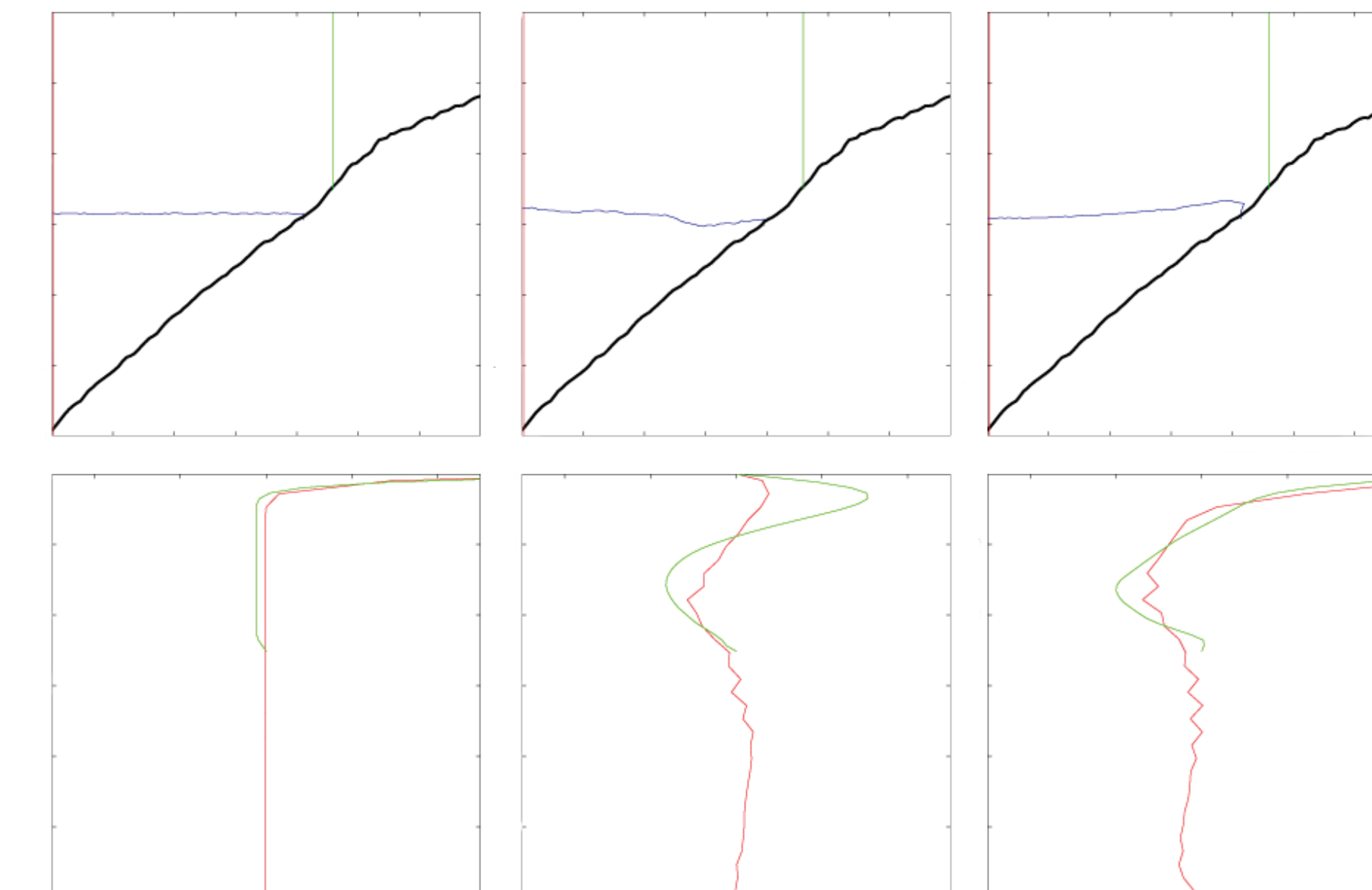


Fig. 3: The position of the pycnocline (top row in blue) and velocity profiles (bottom) for $t = .9, 17.8,$ and 24 hrs with only wind stress acting on the domain. The red and green lines correspond to the data profiles, T-18 and T-91.

One simulation was run such that only wind stress was applied to the domain. Figure 3 shows the position of the pycnocline and the u-profiles for two transects, T-18 and T-91, for several time steps. The two transects are located close to the positions of two of the moorings used by Noble et. al. The similar positions allowed us to verify our results with field data.

Similarly, a wave forced simulation with no wind gives the internal tide at the M2 frequency. Figure 2 illustrates the pycnocline position and u-profiles of the internal wave field at selected time steps. A time series of the shoaling internal wave is shown along with this poster. The maximum penetration, 6050 m, of the pycnocline occurred when only the wave forcing was applied. When the wind was included, the maximum penetration was 6033 m. The maximum penetration for each phasing is shown in Figure 5.

Fig. 4 : The Density Field

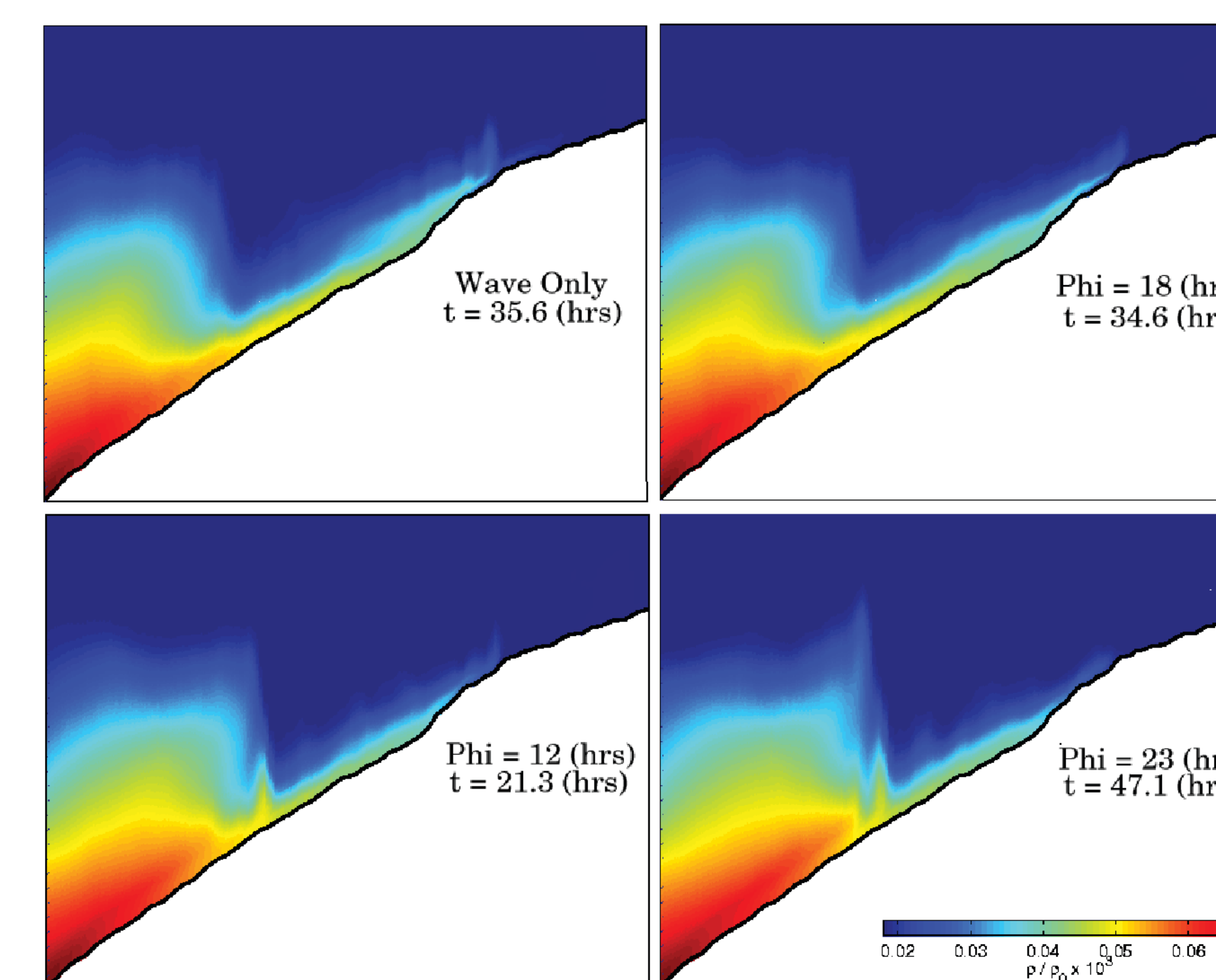


Fig.4: The density field at the timestep of maximum advection where (clockwise from top left) $W_{amp} = W_{avg} = 0$ cm/s, $\phi = 18, \phi = 23$ and $\phi = 12$ (hrs). The legend in the lower right applies to the four frames. The interaction of the wind stress and wave action can be seen in the "lifting" of the density field.

Fig. 5 : Maximum Penetrations

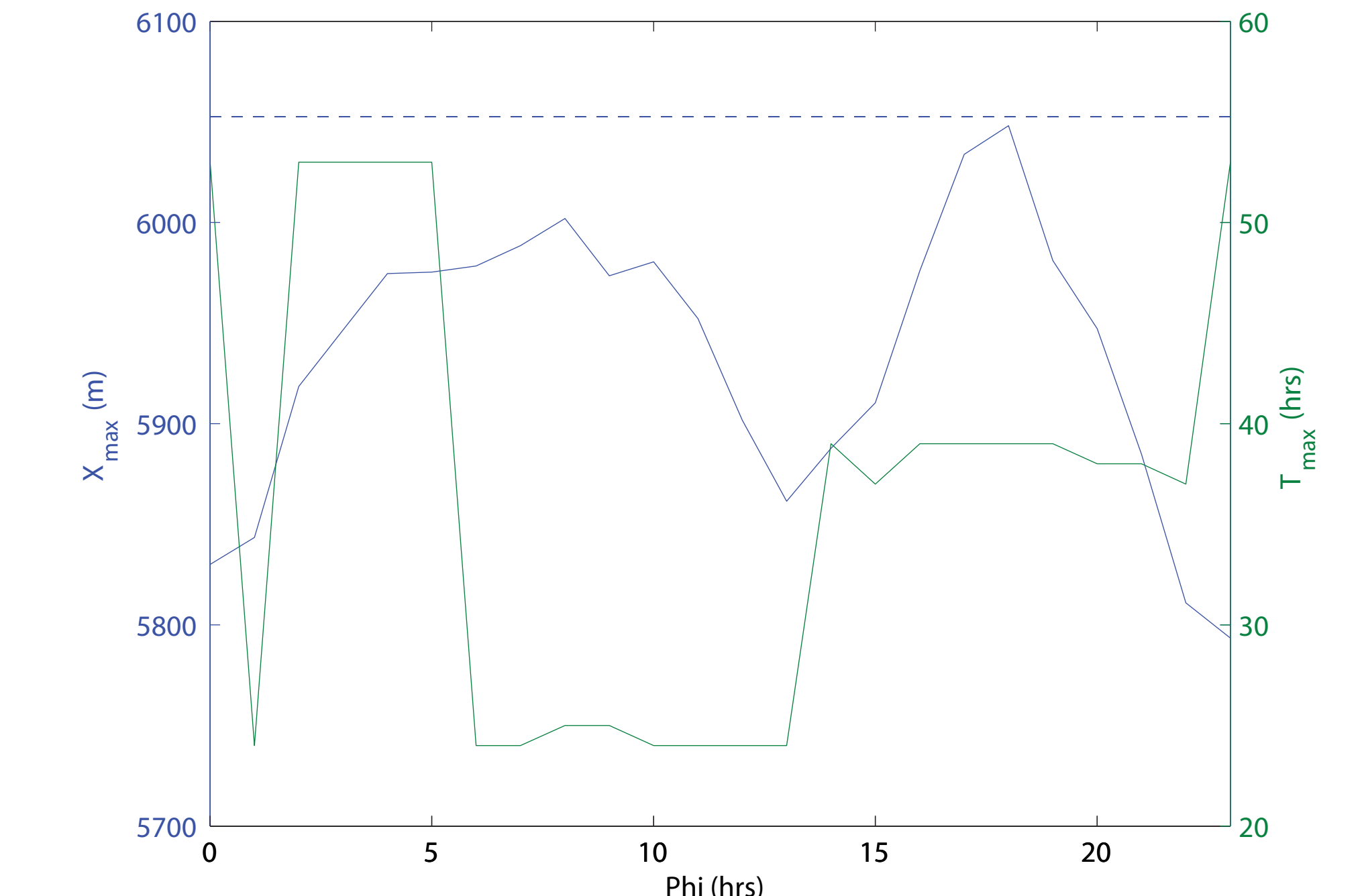


Fig. 5 :The maximum shoreward penetration and the time of that maximum vs. ϕ is above in blue. The green line is the time at which the maximum was reached. The dashed blue line just above 6050 m is the maximum shoreward penetration due to waves only, which occurs at $T \approx 36$ hours.

IV. Conclusion

Figure 5 shows that the shoreward advection of the pycnocline depends on the phasing between the wind and wave forcings. The maximum shoreward penetration when $\phi = 23$ was 5793 m, 259 m less than in the wind only case. The maximum, however, when $\phi = 18$ was almost identical to the wind only case. Further investigation might reveal a relationship between ϕ and x_{max} . In these simulations the wind-forcing restricted shoreward penetration and therefore might limit transport of water near the outfall toward shore. The internal wave field, however, cannot be excluded as a possible transport mechanism as the interaction alters the density field, see Figure 4. Further investigation ought to include the along-shore component of the sea breeze and the associate Eckman Flows.

V. References

- Boehm, A.B., B.F. Sanders, C.D. Winant (2002), *Cross-Shelf Transport at Huntington Beach. Implications for the fate of sewage discharged through an offshore ocean outfall.* Environ. Sci. Technol., 36.9
- Fischer, H., et al. (1979), *Mixing in inland and coastal waters.* Elsevier.
- Noble, M., et al. (2003), *Huntington beach shoreline contamination investigation, phase III,* U.S. Geol. Surv. Open-File Rep. OF 03-0062.
- Zang, Y., R.L. Street, and J.R. Koseff (1994), *A non-staggered grid, fractional step method for time-dependent incompressible Navier-Stokes equations in curvilinear coordinates,* J. Comput. Phys., 114, 18-33

VI. Acknowledgements

Thanks are due to Andrew Bernoff, Karan Venayagamoorthy, Yi-Ju Chou, Jan Wang, and the Stanford EFML. This work was supported by the Harvey Mudd College Center for Environmental Studies.